Available online at www.sciencedirect.com
ScienceDirect
Trans. Nonferrous Met. Soc. China 29(2019) 397−406
Transactions of Nonferrous Metals Society of China
www.tnmsc.cn

Removal and recovery of titanium (IV) from leach liquor of high-sulfur bauxite using calcium alginate microspheres impregnated with di-(2-ethylhexyl) phosphoric acid

Zhen-ning LOU[1,2], Xin XIAO[2], Ying XIONG[2], Yu-chun ZHAI[1]

1. School of Metallurgy, Northeastern University, Shenyang 110819, China;
2. College of Chemistry, Liaoning University, Shenyang 110036, China

Received 4 January 2018; accepted 7 September 2018

Abstract: In the leaching solution of high-sulfur bauxite roasted by sulfuric acid, a high concentration of aluminum presented along with titanium and iron. The present work was to remove Ti(IV) from the leach liquor by calcium alginate microsphere sorbent material (CA-P204) based on natural alginate impregnated with di-(2-ethylhexyl) phosphoric acid (D2EHPA) to purify leaching solution. Cation exchange and chelation make major contributions to the adsorption mechanism according to Fourier-transform infrared spectroscopy and X-ray photoelectron spectroscopy analysis. The results showed that Ti(IV) was successfully removed by the CA-P204 adsorbent from the Ti(IV)−Al(III)−Fe(III) ternary system with a dynamic column experiment. The removal rate of titanium was nearly 95% under optimal conditions and the maximum adsorption capacity was 66.79 mg/g at pH 1.0. Reusability of CA-P204 was evaluated over three consecutive adsorption/desorption cycles. The adsorption process was simple, low-cost, and had no waste discharge, suggesting that the CA-P204 was promising, efficient, and economical for removing Ti(IV) from high-sulfur bauxite leaching solution.

Key words: titanium (IV); D2EHPA; calcium alginate microsphere; high-sulfur bauxite

1 Introduction

High-sulfur bauxite is mainly composed of a high content of Al_2O_3 (from 60% to 65%), accompanied by SiO_2, TiO_2, Fe_2O_3, etc. These impurities will affect the Al extraction process and lower the purity of Al products, among which titanium impurity is one of the important factors. So, it is necessary to study the removal of Ti from the leach liquor of high-sulfur bauxite. Moreover, the efficient separation and recovery of all types of Ti would be beneficial for both economical and sustainability reasons [1,2].

The common methods of removing Ti from leaching solutions are precipitation [3], ion exchange [4], and solvent extraction. Owing to its low operational cost and difficulties, solvent extraction technology has been widely used in the enrichment and separation of Ti at the present state of the hydrometallurgical fields [5−18]. Meanwhile, the extraction efficiency of P204 is very low for Al, making it prefect for separation of Al and Ti. Compared with conventional liquid−liquid extraction that requires a large amount of organics, solid phase extraction (SPE) is now considered to be one of the most promising techniques for pre-concentration, removal, and recovery of metal ions from a wide variety of sources due to its eco-friendliness, speed, simplicity, and low cost [19−22]. Alginate is a natural polysaccharide extracted from algae or bacteria that is cheap, abundant, and biodegradable. Because of its rich hydroxyl and carboxyl groups, alginate and its composites exhibit enhanced adsorption performance, and can be used as an adsorbent or carrier for the recovery of metals from aqueous solutions [23−27]. Although alginate has many advantages, it has solubility in water and needs to be solidified. In addition, the mechanical strength of alginate is not high, and it is necessary to improve its mechanical strength in practical application. Meanwhile, the chemical modification should be used to introduce other functional groups to improve its adsorption performance and selectivity. In our laboratory, algae has been proven to be effective for adsorption, pre-concentration, and separation of Re(VII) and Mo(IV) [28,29].

Foundation item: Project (21201094) supported by the National Natural Science Foundation of China
Corresponding author: Zhen-ning LOU; Tel: +86-24-62207873; E-mail: louzhenning@lnu.edu.cn
DOI: 10.1016/S1003-6326(19)64949-6

In this work, we focused on removal and recovery of Ti(IV) from the leaching solution of calcined high-sulfur bauxite clinker with calcium alginate microspheres impregnated with P204 extractant, designated as CA-P204. The sorbent material was characterized by scanning electron microscopy (SEM), Fourier-transform infrared spectroscopy (FTIR), and X-ray photoelectron spectroscopy (XPS). The effects of pH, contact time, and solid-to-liquid ratio on Ti(IV) adsorption were investigated. The feasibility and practical readiness of the adsorbent for the removal of low concentrations of Ti(IV), in the case of high concentrations of Al(III) and Fe(III), were evaluated by batch and column tests. The preparation of the adsorbent is simple, and this method successfully combines the advantages of solid-phase extraction and liquid–liquid extraction, for which there is no existing literature on the adsorption of Ti.

2 Experimental

2.1 Materials and reagents

Extractant di-(2-ethylheyl) phosphoric acid (P204) was purchased from Alfa Aesar Co. (Shenyang, China, purity >97%), and titanium dioxide from SinoPharm Chemical Reagent Co. (Shenyang, China). A stock solution of Ti was prepared from its oxides via dissolution in concentrated sulfuric acid. Alginate was extracted from natural seaweed. Other reagents were analytical grade and used without further purification. The leaching solution used in this work was obtained from high-sulfur bauxite roasted by sulfuric acid.

2.2 Synthesis of adsorbents

Fresh natural seaweed was washed with tap water to remove sand and other impurities, sun-dried, and crushed. 3 g of seaweed powder was mixed with 30 g of formaldehyde solution (1%, w/v) and 105 g of Na_2CO_3 solution (15 g/L). The resulting mixture was stirred at 323 K to obtain a paste alginate solution. Extractant P204 after saponification with 1 mol/L NaOH (8 mL) was then added into 30 mL of alginate solution and stirred at room temperature for 24 h. Finally, calcium alginate microspheres were formed by dropwise addition of the above mixture into 200 mL of $CaCl_2$ solution (0.5 mol/L) through a syringe. The suspension was then stirred at 303 K for 24 h. The obtained gel beads were filtered and washed with deionized water several times, and then dried overnight at 323 K, as shown in Scheme 1. The adsorbent was abbreviated as CA-P204. Similarly, CA was the pure calcium alginate instead of containing P204 for the comparison.

2.3 Characterization

The pH of the solution was measured with S-3C model pH meter, while the concentrations of metal ions were measured using PE optima 8000 model atomic emission spectrophotometer. Analysis of the morphology was carried out using a scanning electron microscope (Philips XL 30, The Netherlands). FTIR spectra were recorded on a Nicolet 5700 FTIR spectrophotometer. XPS spectra were measured using a Thermo ESCALAB 250 X-ray photoelectron spectrometer with an Al K_α X-ray source and were fitted using XPS PEAK4.1 software.

2.4 Batch adsorption studies

All equilibrium adsorption experiments were individually conducted in a temperature-controlled shaker at a speed of 180 r/min for 24 h at (303±1) K. Adsorption capacity for Ti(IV) was measured with 10 mg of adsorbent in 5 mL of Ti(IV) solution in single solution. The effect of acidity on Ti(IV) adsorption was

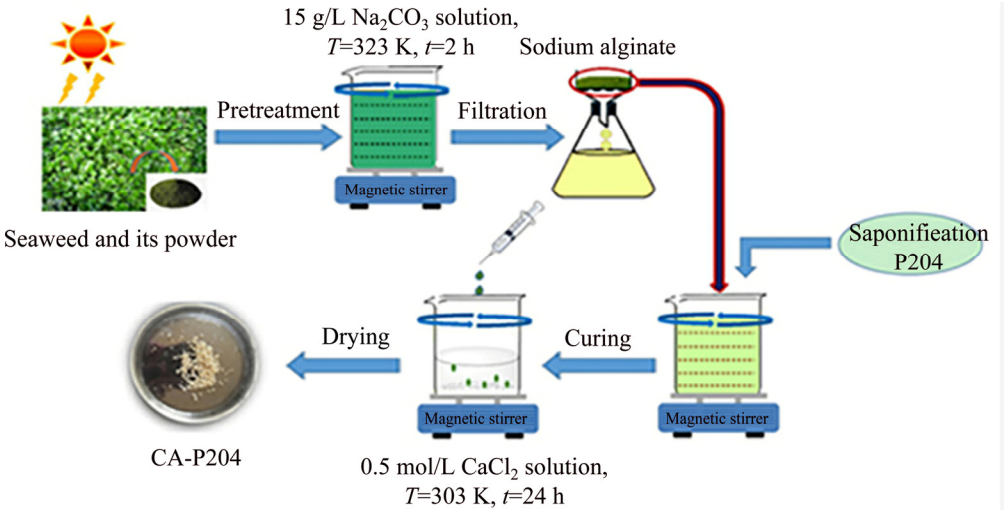

Scheme 1 Preparation flow of CA-P204

studied using 20 mg/L of initial Ti concentration from pH 1.25 to 3 mol/L in a 10 mL flask. The adsorption kinetics for Ti(IV) was measured by adding 10 mg of dry adsorbents to 5 mL of Ti(IV) solution (20 mg/L in sulfuric acid at pH 1) at 293, 303, 313 and 323 K, respectively. After adsorption reached equilibrium, the metal ion concentration was measured. The percentage adsorption was calculated according to

$$A=\frac{(C_{\mathrm{i}}-C_{\mathrm{e}})}{C_{\mathrm{i}}}\times 100\% \quad (1)$$

where C_{i} and C_{e} are the initial and equilibrated metal ion concentrations (mg/L), respectively.

2.5 Column experiments: Loading, elution, and regeneration

Column experiments were carried out in a glass column (250 mm in height, 7.8 mm in inner diameter). The column was conditioned with 0.1 mol/L H_2SO_4 (pH 0.85, the same pH as the leachate) for 1 h. After rinsing with acid, approximately 100 mg of CA-P204 was packed onto the glass column. The bauxite leaching solution ($C_{\mathrm{Ti(IV)}}$=220 mg/L, $C_{\mathrm{Fe(III)}}$=780 mg/L, $C_{\mathrm{Al(III)}}$=2440 mg/L, pH 0.85) was fed from the top onto the column using a peristaltic pump. The adsorbed Ti(IV) ions were eluted with a mixture of 2 mol/L H_2SO_4 and 3% H_2O_2, and Fe(III) ions were eluted with 6 mol/L HCl, respectively. The velocity for the adsorption and desorption tests was maintained at 8.02 mL/h. The effluent solution was collected continuously at 30 min intervals, and the concentration of each metal was determined by inductively coupled plasma atomic emission spectroscopy (ICP-AES). To test the reusability of the CA-P204, consecutive adsorption–desorption cycles were repeated three times.

2.6 Ti speciation analysis in sulfuric acid solution

The speciation of Ti directly affects its adsorption behavior. The test solution is sulfuric acid as the leach liquor of high-sulfur bauxite is roasted by sulfuric acid. The speciation of Ti in a sulfuric acid system consists of cationic, anionic, and neutral complexes [30,31]. TiO^{2+} has been reported as a predominant species at low acidities ($[H^+]\leq 0.5$ mol/L) [8,18]. Distribution curve of each speciation at 298 K was obtained by the formation constants of Ti(IV) with HSO_4^-, SO_4^{2-} and H_2O in different concentrations of sulfuric acid solution after calculation. As can be seen from Fig. 1, the concentrations of various species at pH<1 followed the order $[TiO^{2+}] > [Ti(OH)_3HSO_4] > [Ti(OH)_2^{2+}] > [TiOHSO_4^+] > [TiO(SO_4)_2^{2-}]$, suggesting that the dominant species of Ti(IV) was TiO^{2+} in the low concentration sulfate leaching solution.

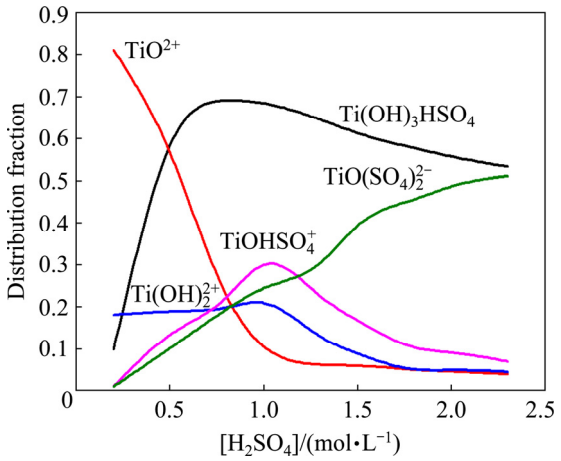

Fig. 1 Species distribution of Ti(IV) in sulfate solution

3 Results and discussion

3.1 Characterization of adsorbent

A SEM analysis was carried out to determine the change in morphology before and after impregnation of P204, as shown in Fig. 2. According to the SEM images, the morphologies showed significant difference between CA and CA-P204. The surface of CA was porous, rough,

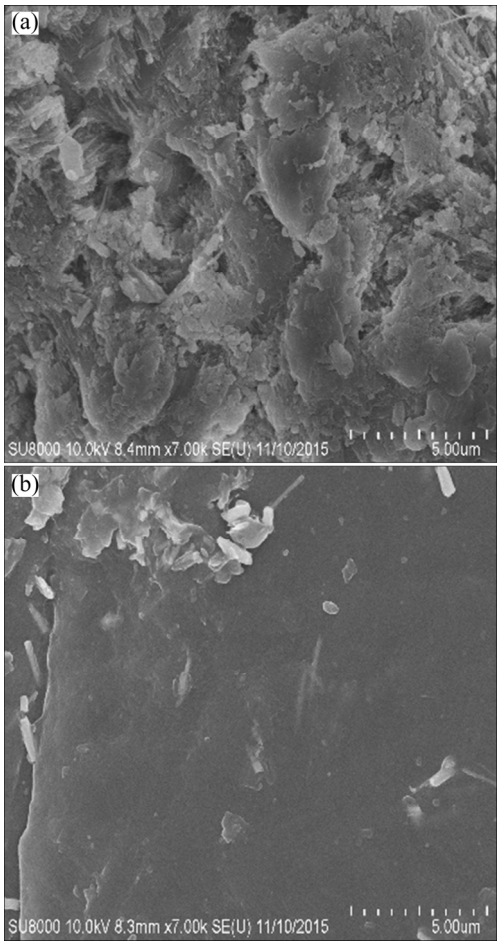

Fig. 2 SEM images of CA (a) and CA-P204 (b)

and irregular, while the surface of CA-P204 was very smooth and the cavity almost disappeared, which may be due to P204 coverage on the CA surface.

The functional group changes of P204 were examined by FTIR spectroscopy, providing evidence of molecular interaction. A comparison of FTIR spectra of CA, P204, and CA-P204 before and after adsorption is shown in Fig. 3. As shown in Figs. 3(b) and (c), the characteristic bands of P204 at 1681 cm^{-1} (δ_{P-OH}), 1234 cm^{-1} ($\nu_{P=O}$), 1032 cm^{-1} (ν_{P-O-C}), and 2800−2900 cm^{-1} (ν_{C-H}) were observed in the CA-P204 spectra, indicating the presence of P204 on the CA gel beads. These observations suggest that CA-P204 adsorbent was successfully synthesized.

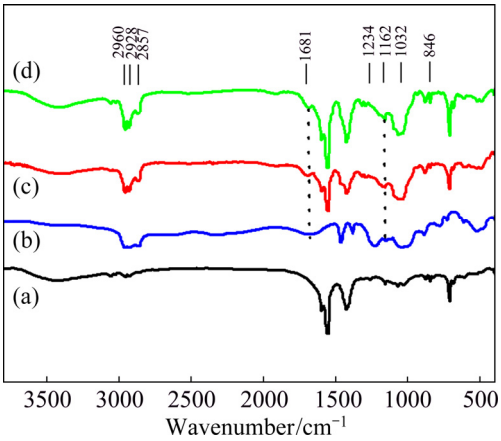

Fig. 3 FTIR spectra of CA (a), P204 (b), CA-P204 (c), and CA-P204 loaded with Ti(IV) (d)

3.2 Influence of acidity and solid−liquid ratio on adsorption of Ti(IV)

The acidity of the solution is the most important factor in the adsorption process because it can affect not only the adsorption efficiency of the adsorbent, but also the speciation of the adsorbate. The effect of the initial acidity on the adsorption of Ti(IV) was examined in the range of pH 1.25 to $[H^+]$=3 mol/L, and the results are shown in Fig. 4(a). It was found that approximately 95% adsorption of Ti(IV) was achieved by CA-P204 at pH 1.00, but it was not adsorbed by CA at any acidities. With increasing acidity, the adsorption percentage of CA-P204 decreased to a minimum at pH 0.5, and gradually increased to a second maximum peak at 1 mol/L at which the adsorption percentage reached approximately 85%. The acidity of the actual leachate was pH 0.85, and the adsorption percentage of Ti(IV) could also reach greater than 90%.

The effect of solid−liquid ratio on the adsorption of Ti(IV) in the leaching solution of bauxite was studied, and the results are shown in Fig. 4(b). With increasing solid−liquid ratio, the adsorption percentage of Ti(IV) increased gradually, and the maximum adsorption of Ti(IV) was approximately 93% at a solid−liquid ratio of 18:1 g/L. However, when the solid−liquid ratio was 16:1 g/L, the loss of Al(III) was the smallest (10%) and the adsorption percentage of Fe(III) was approximately 48%. The selectivity factors were calculated by

$$S_{Ti/X} = \lg \frac{(q_e/C_e)_{Ti}}{(q_e/C_e)_X} \quad (2)$$

where q_e denotes the adsorption capacity measured after adsorption, X denotes Fe(III) or Al(III), and $S_{Ti/X}$ represents adsorption selectivity for Ti(IV) over X. The selectivity factors $S_{Ti/Al}$ and $S_{Ti/Fe}$ were 1.62 and 0.92 at a solid−liquid ratio of 16:1 g/L, respectively, indicating that Ti(IV) and Al(III) could be separated, but that Ti(IV) and Fe(III) were inseparable under current conditions.

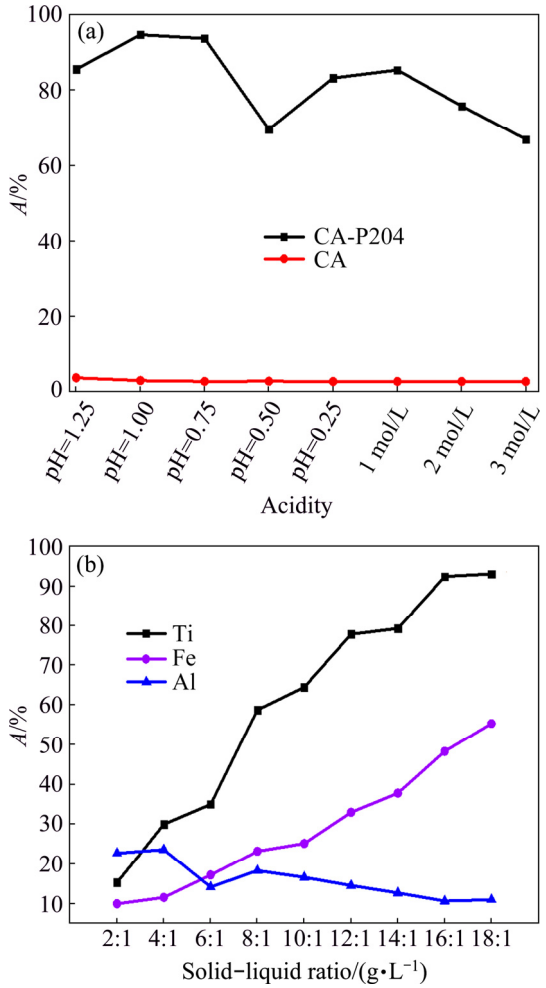

Fig. 4 Effect of acidity on adsorption of Ti(IV) in single system ([Ti(IV)]=20 mg/L; solid−liquid ratio=2:1 g/L; temperature=303 K; shaking time=24 h) (a) and solid−liquid ratio on adsorption of Ti(IV) in bauxite leaching solution ([Ti(IV)]=220 mg/L; [Fe(III)]=780 mg/L; [Al(III)]=2440 mg/L; temperature=303 K; shaking time=24 h) (b)

3.3 Adsorption isotherms

Adsorption isotherms were used to characterize the

interaction of Ti(IV) ions with the adsorbent, which were performed at 303 K and the results are shown in Fig. 5(a). When the equilibrium concentration of metal ions increased gradually, the adsorption capacity increased until reaching a constant. The Langmuir, Freundlich, and Temkin models were used for describing the adsorption behavior. All the isotherm model parameters for the Ti(IV) adsorption are summarized in Table 1. According to the values of the correlation coefficients (R^2), the Langmuir adsorption isotherm fitted the experimental data well. A reasonable explanation for this is that Ti(IV) ions in the aqueous solution were monolayer-adsorbed onto the surface of the CA-P204. The maximum adsorption capacity of Ti(IV) calculated from the Langmuir isotherm equation was 66.79 mg/g.

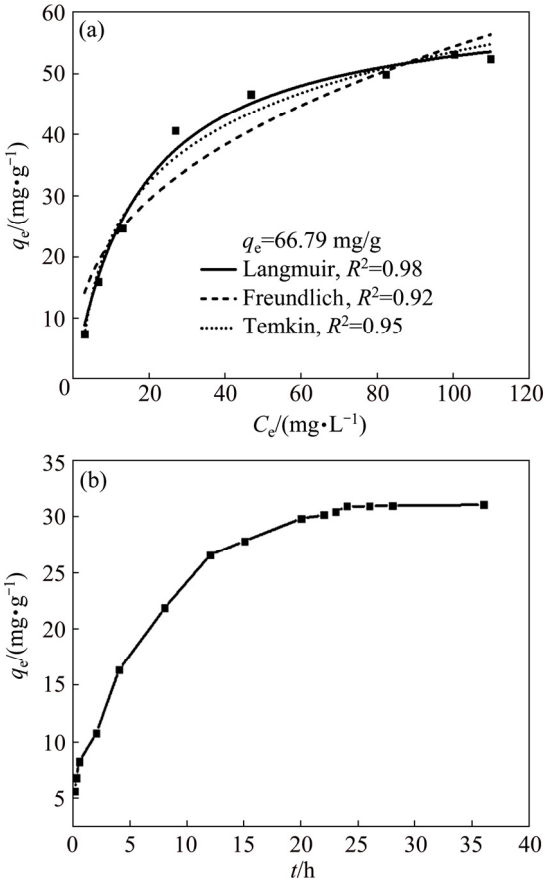

Fig. 5 Adsorption isotherms for Ti(IV) on CA-P204 (a) and effect of time on adsorption of Ti(IV) (b) (C_0=20 mg/g; solid−liquid ratio=2:1 g/L; temperature=303 K; shaking time=72 h)

Table 1 Adsorption isotherm constants for Ti(IV) on CA-P204

Isotherm		Constant	
Langmuir	$q_e=\frac{q_{max}K_LC_e}{1+K_LC_e}$	q_{max}/(mg·g^{-1})	66.79
		K_L/(L·mg^{-1})	0.13
		R^2	0.98
Freundlich	$q_e=K_FC_e^{1/n}$	K_F/(L·mg^{-1})	13.01
		n	3.31
		R^2	0.92
Temkin	$q_e=\frac{RT}{b}\ln(A_TC_e)$	A_T/(L·g^{-1})	3.22
		b	285.54
		R^2	0.95

3.4 Adsorption kinetics and thermodynamics

The kinetics of Ti(IV) adsorption was investigated in single solution, with contact time ranging from 5 min to 36 h, as shown in Fig. 5(b). It can be seen that the adsorption capacity increased with time and reached adsorption equilibrium after 24 h. The pseudo-first-order (Eq. (3)), pseudo-second-order (Eq. (4)), Elovich (Eq. (5)), and intraparticle diffusion (Eq. (6)) kinetic models were applied to the experimental data to analyze the adsorption kinetics:

$$\lg(q_e-q_t)=\lg q_e-\frac{k_1}{2.303}t \quad (3)$$

$$\frac{t}{q_t}=\frac{1}{k_2q_e^2}+\frac{1}{q_e}t \quad (4)$$

$$q_t=\frac{1}{\beta}\ln(\alpha\beta)+\frac{1}{\beta}\ln t \quad (5)$$

$$q_t=k_pt^{0.5}+C \quad (6)$$

where q_e (mg/g) and q_t (mg/g) represent the adsorption amount of metal ions at equilibrium and at any given time t, respectively. k_1 (h^{-1}) and k_2 (g/(mg·h)) are the rate constants of the pseudo-first-order and pseudo-second-order models, respectively. The parameter α (mg/(g·h)) represents the initial adsorption rate constant, and β (g/mg) is a constant associated with the extent of surface coverage and activation energy for chemisorption, and k_p (mg/(g·h$^{1/2}$)) represents the particle diffusion rate constant. The corresponding kinetic parameters and the determination coefficient (R^2) are listed in Table 2. Higher correlation coefficient values of the pseudo-second-order model suggested that the pseudo-second-order equation fitted the experimental data better. Moreover, the adsorption rate for the pseudo-second-order model reached the maximum (0.41 g/(mg·h)) at 303 K.

Thermodynamic parameters, such as the Gibbs free energy change (ΔG^Θ), enthalpy change (ΔH^Θ), and entropy change (ΔS^Θ) for the adsorption systems, were calculated using the equations described in our previous work [32] and are shown in Table 3. The negative values of ΔG^Θ at 293, 303, 313 and 323 K confirmed that the adsorption process was spontaneous in nature. At the same time, it can be seen that positive values of ΔH^Θ (4.95 kJ/mol) and ΔS^Θ (33.90 J/(mol·K)) were obtained, suggesting that the adsorption process was an endothermic and spontaneous reaction with increased randomness in nature.

Table 2 Comparison of adsorption kinetic constants at different temperatures

T/K	q_e/(mg·g^{-1})	Pseudo-first-order			Pseudo-second-order			Elovich			Intraparticle diffusion	
		q_e/(mg·g^{-1})	k_1/h^{-1}	R^2	q_e/(mg·g^{-1})	k_2/(g·mg^{-1}·h^{-1})	R^2	α/(mg·g^{-1}·h^{-1})	β/(g·mg^{-1})	R^2	k_p/(mg·g^{-1}·h$^{-1/2}$)	R^2
293	26.74	28.50	1.37	0.76	33.23	0.18	0.94	29.38	0.199	0.88	6.34	0.92
303	31.01	31.35	0.21	0.95	32.99	0.41	0.99	75.62	0.213	0.89	4.98	0.93
313	25.61	25.60	0.19	0.86	30.55	0.33	0.97	42.22	0.203	0.93	5.98	0.90
323	32.48	31.19	0.16	0.98	38.18	0.19	0.99	36.5	0.16	0.94	6.19	0.89

Table 3 Thermodynamic parameters of Ti(IV) adsorption on CA-P204 adsorbent

T/K	ΔG^{Θ}/(kJ·mol^{-1})	ΔH^{Θ}/(kJ·mol^{-1})	ΔS^{Θ}/(J· mol^{-1}·K^{-1})
293	−4.98	4.95	33.90
303	−5.32	4.95	33.90
313	−5.66	4.95	33.90
323	−6.00	4.95	33.90

3.5 Desorption of Ti(IV)

To regenerate the adsorbent, the effect of stripping agents and their concentrations on Ti desorption was studied, and the results are listed in Table 4. Mixtures of H_2SO_4 with a certain amount of H_2O_2 could quantitatively strip Ti due to the formation of $Ti(OH)_2(H_2O_2)SO_4$ [1]. It was observed that the desorption efficiency increased with H_2SO_4 concentration increasing from 1 to 2 mol/L. However, there was a decrease when the H_2SO_4 concentration was 3 mol/L. Similarly, with the increase of H_2O_2 mass fraction, the elution efficiency was significantly improved. Thus, 2 mol/L H_2SO_4 and 3% H_2O_2 solution could be used as an eluted agent, and the elution efficiency was 98.56% for Ti(IV).

Table 4 Desorption of loaded Ti(IV) on CA-P204 adsorbent

Eluent	Elution efficiency/%
1 mol/L H_2SO_4−1%H_2O_2	66.51
1 mol/L H_2SO_4−2%H_2O_2	88.12
1 mol/L H_2SO_4−3%H_2O_2	90.23
2 mol/L H_2SO_4−1%H_2O_2	67.19
2 mol/L H_2SO_4−2%H_2O_2	93.25
2 mol/L H_2SO_4−3%H_2O_2	98.56
3 mol/L H_2SO_4−1%H_2O_2	62.65
3 mol/L H_2SO_4−2%H_2O_2	78.29
3 mol/L H_2SO_4−3%H_2O_2	80.75

3.6 Column-mode adsorption and regeneration of CA-P204

In order to improve the removal efficiency of Ti(IV) from high concentration Al(III) (C_{Al}=2440 mg/L) and Fe(III) (C_{Fe}=780 mg/L) leaching solution and examine the reusability of the prepared adsorbent, three successive adsorption–desorption cycles were performed using a glass column with an amount of the CA-P204 as adsorbent (the experimental installation is shown in Fig. 6(a)). As shown in Table 5, Al(III) was not adsorbed on the CA-P204, and a certain amount of Ti(IV) and Fe(III) were adsorbed simultaneously. Although some iron was co-adsorbed by CA-P204, 6 mol/L HCl was used to strip Fe(III) before stripping Ti(IV) (the adsorption−desorption cycle process chart is shown in Fig. 6(b)). The maximum adsorption capacities of Ti(IV) on the CA-P204 adsorbent for three successive column cycles were calculated as 158.40, 61.17, and 124.93 mg/g, respectively. The second adsorption amount of adsorbents for Ti(IV) was much smaller than that of the first and third adsorption. The possible reason is that when the leaching solution flows through the column, Ti(IV) is adsorbed initially at the top of column. As the volume of the leaching solution increases, the Ti(IV) adsorbed on the head of column further increases, and a portion of Ti(IV) is likely to enter into the internal structure of the adsorbent, which is not easy to elute. This leads to the reduction of the adsorption site, so the adsorption capacity of the second adsorption is less than those of the other two cycles.

The breakthrough curves of the bauxite leaching solution after three successive adsorption–desorption cycles are shown in Fig. 7. It was observed that Ti(IV)

Table 5 Performance of CA-P204 packed into fixed-bed column for three consecutive adsorption–elution cycles

Cycle No.	Mixture solution	Adsorbing capacity/(mg·g^{-1})	Elution efficiency/% (2 mol/L H_2SO_4− 3% H_2O_2)
1	Ti(IV), 220 mg/L	158.40	85.80
	Fe(III), 780 mg/L	29654.1	0.11
	Al(III), 2440 mg/L	0	0
2	Ti(IV), 220 mg/L	61.17	108.89
	Fe(III), 780 mg/L	21269.68	0.14
	Al(III), 2440 mg/L	0	0
3	Ti(IV), 220 mg/L	124.93	87.95
	Fe(III), 780 mg/L	176.51	0.15
	Al(III), 2440 mg/L	0	0

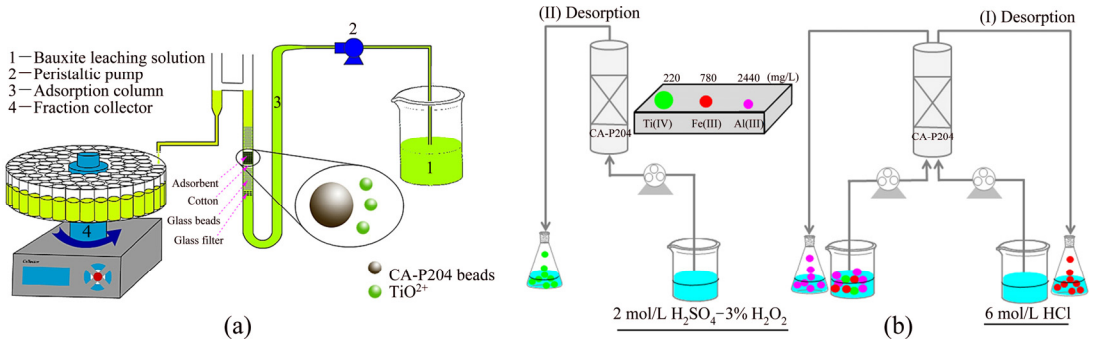

Fig. 6 Column experiment installation (a) and adsorption−desorption cycle process chart (b)

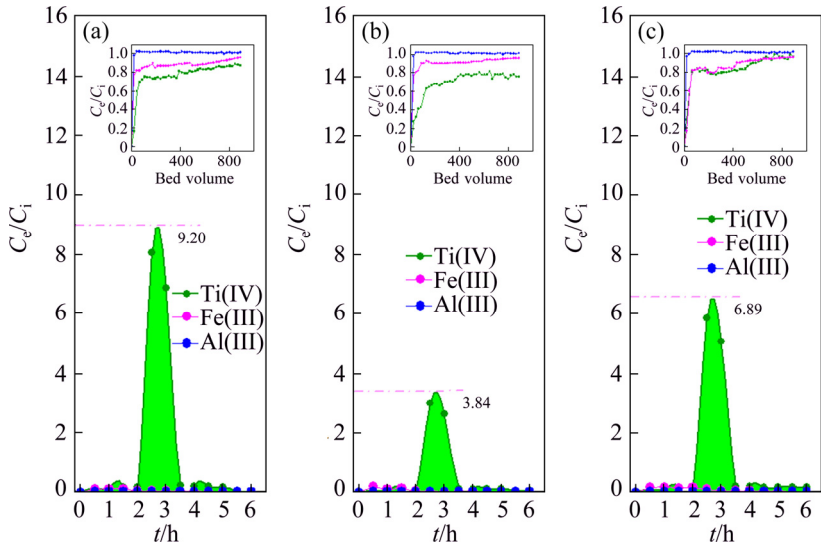

Fig. 7 Effect of successive adsorption–desorption cycle on breakthrough curve for removal of Ti(IV) from bauxite leaching solution (Ti(IV)=220 mg/L; Fe(III)=780 mg/L; Al(III) =2240 mg/L; temperature=303 K; flow rate=8.02 mL/h): (a) Cycle 1; (b) Cycle 2; (c) Cycle 3

was enriched efficiently, and the pre-concentration factors were 9.20 for cycle 1, 3.84 for cycle 2, and 6.89 for cycle 3. According to the area of the curves, 85.80%−108.89% Ti(IV) was eluted for three cycles. In order to further prove the stability and recycling performance of the adsorbent, phosphorus contents on the CA-P204 adsorbent before and after three successive adsorption–desorption cycles were also determined by ICP-AES, which were 14.09 and 12.93 mg/L, respectively. A small decrease of phosphorus content indicated that the extractant P204 on the calcium alginate surface was stable and that CA-P204 could be used repeatedly at least three times.

3.7 Adsorption mechanism

According to the above discussion of the characteristics of the adsorbents, it was found that the CA-P204 adsorbent had P═O and P—OH groups. Comparing Figs. 3(c) to (d) shows that the intensities of the P—OH bands at 1681 cm^{-1} decreased, and that the P═O absorption band bonded to the Ti(IV) shifted from 1234 to 1162 cm^{-1} after adsorption. Simultaneously, the band at 846 cm^{-1} appeared in Fig. 3(d), which probably resulted from the Ti—O—Ti bridging bond. All these phenomena indicate that these groups were involved in the adsorption of TiO^{2+} by cation exchange and chelation.

To further confirm the adsorption mechanism, XPS analysis was performed, and the results are presented in Fig. 8. The wide-scan XPS spectra for CA-P204 and CA-P204 loaded with Ti(IV) are shown in Fig. 8(a). It is clear that new peaks at binding energies (BEs) of 459.30 and 465.03 eV appeared after Ti(IV) adsorption, which provides evidence of Ti(IV) adsorbed on the surface of the adsorbent. Moreover, the O 1s and P 2p spectra could be deconvoluted into four (O—P, O═P, O—Ti, and O—R) and three (P—O, P═O, and P—OR) individual component peaks after Ti(IV) adsorption, as shown in Figs. 8(c) and (e), respectively. The BE of O—P shifted from 532.56 to 531.16 eV, and the relative content of O—P decreased from 32.05% to 12.07% after adsorption, which might be due to changes in the density of the electron cloud around oxygen atoms because of the generation of a new O—Ti bond, as shown in Figs. 8(b) and (c). In addition, the BEs of P—O and P═O shifted from 134.21 to 132.88 eV and from 134.53 to 133.43 eV,

respectively. An increase or a decrease in the relative content of P—O (from 10.23% to 19.52%) or P═O (from 48.54% to 38.59%) also indicated that they were involved in the adsorption of Ti(IV), as shown in Figs. 8(d) and (e). Thus, the adsorption mechanism of Ti(IV) on the CA-P204 adsorbent may be attributed to cation exchange and chelation, as shown in Scheme 2.

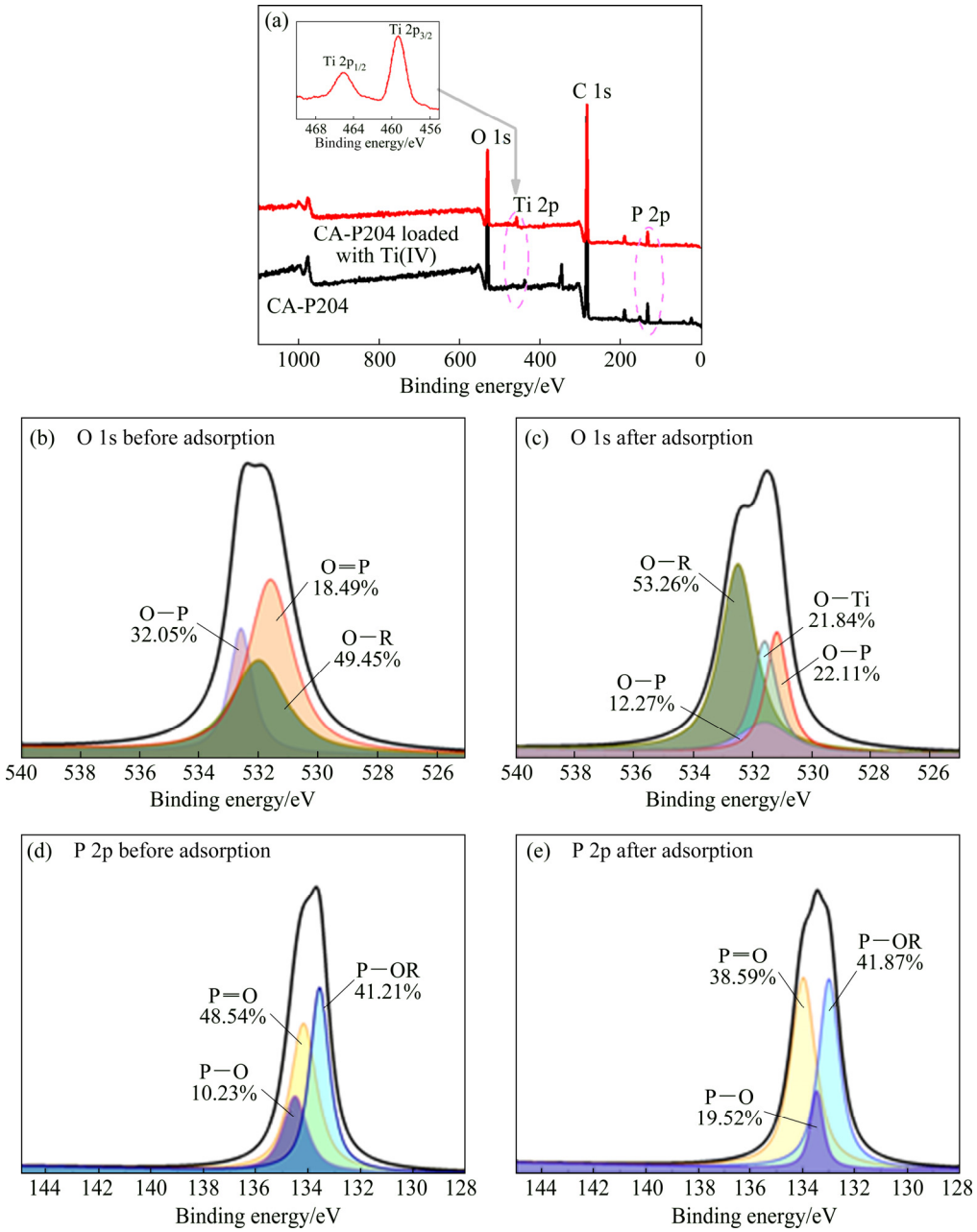

Fig. 8 XPS spectra of CA-P204 before and after Ti(IV) adsorption (a), O 1s spectra before Ti(IV) adsorption (b), O 1s spectra after Ti(IV) adsorption (c), P 2p spectra before Ti(IV) adsorption (d) and P 2p spectra after Ti(IV) adsorption (e)

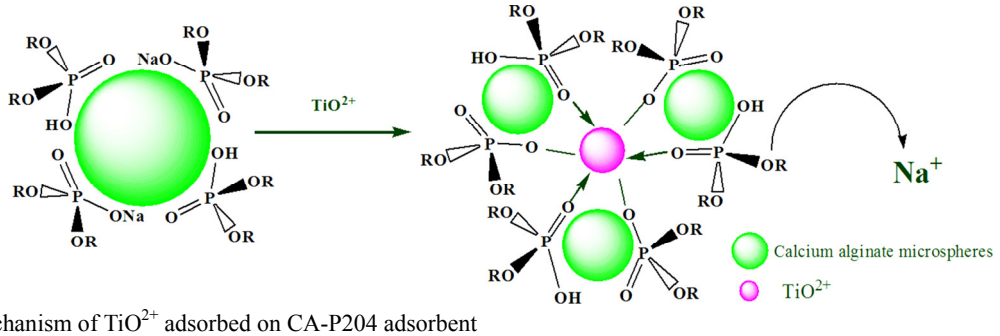

Scheme 2 Mechanism of TiO^{2+} adsorbed on CA-P204 adsorbent

4 Conclusions

(1) Ti(IV) was successfully removed from high-sulfur bauxite leaching solution containing high concentrations of Al(III) and Fe(III) by calcium alginate microspheres impregnated with extractant P204. The maximum adsorption capacity for Ti(IV) was 66.79 mg/g at pH 1.0. The P═O and P—O functional groups were confirmed to participate in the coordination and cation exchange by FTIR and XPS analysis.

(2) The adsorption process followed the monolayers Langmuir isotherm model and the pseudo-second-order kinetics equation. Thermodynamic parameters indicated that the adsorption process was an endothermic reaction and the randomness increased.

(3) The effectiveness of the removal of Ti(IV) from a Ti(IV)−Al(III)−Fe(III) mixture solution was tested by three successive column cycle experiments. Although Fe(III) was co-adsorbed, the separation of Fe(III) and Ti(IV) could be achieved by step elution with different eluents. At the same time, Al(III), Fe(III), and Ti(IV) could be recovered separately. All these results suggest that the removal of Ti (IV) by CA-P204 could be a viable method for the purification of leach liquor.

(4) The main advantages of the process were its simplicity, low cost, environmental safety, and significantly reduced final waste emissions.

References

[1] ZHU Zhao-wu, ZHANG Wen-sheng, CHENG Chu-yong. A literature review of titanium solvent extraction in chloride media [J]. Hydrometallurgy, 2011, 105: 304−313.

[2] MENG Fan-cheng, XUE Tian-yan, LIU Ya-hui, ZHANG Guo-zhi, QI Tao. Recovery of titanium from undissolved residue (tionite) in titanium oxide industry via NaOH hydrothermal conversion and H_2SO_4 leaching [J]. Transactions of Nonferrous Metals Society of China, 2016, 26: 1696−1705.

[3] GERASIMOVA L, MASLOVA M. Precipitation of titanium(IV) and iron(III) phosphates from sulfuric acid solutions [J]. Russian Journal of Applied Chemistry, 2003, 76: 1855−1857.

[4] KIRIYAMA T, HARAGUCHI M, KURODA R. Combined anion-exchange separation and spectrophotometric determination of traces of titanium in sea water [J]. Fresenius Zeitschrift Für Analytische Chemie, 1981, 307: 352−355.

[5] HAO Xiao-li, LU Li, LIANG Bin, LI Chun, WU Pan. Solvent extraction of titanium from the simulated ilmenite sulfuric acid leachate by trialkylphosphine oxide [J]. Hydrometallurgy, 2012, s113−114: 185−191.

[6] BISWAS R K, KARMAKAR A K. Solvent extraction of Ti(IV) in the Ti(IV)− SO_4^{2-} (H^+,Na^+)−Cyanex302−kerosene−5% (v/v) hexan-1-ol system [J]. Hydrometallurgy, 2013, 1−10: 134−135.

[7] ALLAL K M, HAUCHARD D, STAMBOULI M, PAREAU D, DURAND G. Solvent extraction of titanium by tributylphosphate, trioctylphosphine oxide and decanol from chloride media [J]. Hydrometallurgy, 1997, 45: 113−128.

[8] KATHRYN C S. Recovery of titanum from the leach liquors of titaniferous magnetites by solvent extraction: Part 1. Review of the literature and aqueous thermodynamics [J]. Hydrometallurgy, 1999, 51: 239−253.

[9] ISLAM M F, BISWAS R K. Solvent Extraction of Ti(IV), Fe(III) and Fe(II) from acidic sulphate medium with di-o-tolyl phosphori c-benzene-hexan-1-ol system: A separation and mechanism study [J]. Hydrometallurgy, 1985, 13: 365−376.

[10] SEYFI S, ABDI M. Extraction of titanium(IV) from acidic media by tri-n-butyl phosphate in kerosene [J]. Minerals Engineering, 2009, 22: 116−118.

[11] WANG Qi, JIANG Lin, NI Fan, WANG Tao. The separation and concentration of titanium(IV) from sulfuric acid solution with trioctylamine [J]. Industrial & Engineering Chemistry Research, 2012, 51: 3430−3435.

[12] TAICHI S, TAKATO N. The extraction of titanium(IV) and aluminium(III) from sulphuric acid solutions by di-(2-ethylhexyl)-phosphoric acid [J]. Analytica Chimica Acta, 1975, 76: 401−408.

[13] SILVA G C D, DWECK J, AFONSO J C. Liquid–liquid extraction (LLE) of iron and titanium by bis-(2-ethyl-hexyl) phosphoric acid (D2EHPA) [J]. Minerals Engineering, 2008, 21: 416−419.

[14] BISWAS R K, BEGUM D A. Solvent extraction of tetravalent titanium from chloride solution by di-2-ethylhexyl phosphoric acid in kerosene [J]. Hydrometallurgy, 1998, 49: 263−274.

[15] BISWAS R K, ZAMAN M R, ISLAM M N. Extraction of TiO_2^+ from 1M (Na^+, H^+) SO_4^{2-} by D2EHPA [J]. Hydrometallurgy, 2002, 63: 159−169.

[16] PHALKE P N, SHERIKAR A V, DHADKE P M. Extraction of titanium(IV) from sulphate media with bis-2-ethyl hexyl phosphoric acid [J]. Indian Journal of Chemistry Section A, 1997, 36: 446−448.

[17] SINGH R K, DHADKE P M. Extraction and separation of titanium(IV) with D2EHPA and PC-88A from aqueous perchloric acid solutions [J]. Journal of the Serbian Chemical Society, 2002, 67: 507−521.

[18] SAJI J, REDDY M L P. Selective extraction and separation of titanium(IV) from multivalent metal chloride solutions using 2-ethylhexyl phosphonic acid mono 2-ethylhexyl ester [J]. Separation Science & Technology, 2003, 38: 427−441.

[19] YAN Ping, HE Man, CHEN Bei-bei, HU Bin. Fast preconcentration of trace rare earth elements from environmental samples by di(2-ethylhexyl)phosphoric acid grafted magnetic nanoparticles followed by inductively coupled plasma mass spectrometry detection [J]. Spectrochimica Acta, Part B: Atomic Spectroscopy, 2017, 136: 73−80.

[20] MENDOZA-REYES L G, GYVESS J D. Novel D2EHPA-polysiloxane-based sorbent for titanium(IV) extraction and separation [J]. Journal of the Mexican Chemical Society, 2011, 55: 72−78.

[21] BARMAN M K, SRIVASTAVA B, CHATTERJEE M, MANDAL B. Solid-phase extraction, separation and preconcentration of titanium(IV) with SSG-V10 from some other toxic cations: A molecular interpretation supported by DFT [J]. RSC Advances, 2014, 4: 33923−33934.

[22] WU Dong-bei, SUN Yan-hong, WANG Qi-gang. Adsorption of lanthanum (III) from aqueous solution using 2-ethylhexyl phosphonic acid mono-2-ethylhexyl ester-grafted magnetic silica nanocomposites [J]. Journal of Hazardous Materials, 2013, 260: 409−419.

[23] HUANG Yan-jun, WU Hai-ling, SHAO Tai-kang, ZHAO Xia, PENG Hong, GONG Yue-fa, WAN Hui-hai. Enhanced copper adsorption by DTPA-chitosan/alginate composite beads: Mechanism and application in simulated electroplating wastewater [J]. Chemical Engineering Journal, 2018, 339: 322−333.

[24] VIJAYALAKSHMI K, MAHALAKSHMI B D, SRINIVASAN L, THANDAPANI G, SUDHA P N, VENKATESAN J, SUKUMARAN A. Batch adsorption and desorption studies on the removal of lead (II) from aqueous solution using nanochitosan/sodium alginate/ microcrystalline cellulose beads [J]. International Journal of Biological Macromolecules, 2017, 104: 1483−1494.
[25] GOKILA S, GOMATHI T, SUDHA P N, SUKUMARAN A. Removal of the heavy metal ion chromium(VI) using Chitosan and Alginate nanocomposites [J]. International Journal of Biological Macromolecules, 2017, 104: 1459−1468.
[26] MOHAMAD A F, ZOHREH M, ANI I. Mass transfer kinetics of Cd(II) ions adsorption by titania polyvinylalcohol−alginate beads from aqueous solution [J]. Chemical Engineering Journal, 2017, 308: 700−709.
[27] WANG Fu-chun, ZHAO Jun-mei, LI Wen-song, ZHOU Hua-cong, YANG Xing-fu, SUI Na, LIU Hui-zhou. Preparation of several alginate matrix gel beads and their adsorption properties towards rare earths (III) [J]. Waste Biomass Valor, 2013, 4: 665−674.
[28] XIONG Ying, XU Jia, SHAN Wei-jun, LOU Zhen-ning, FANG Da-wei, ZANG Shu-liang, HAN Guang-xi. A new approach for rhenium(VII) recovery by using modified brown algae Laminaria japonica adsorbent [J]. Bioresource Technology, 2013, 127: 464−472.
[29] LOU Zhen-ning, WANG Jing, JIN Xu-dong, WAN Li, WANG Yue, CHEN Hui, SHAN Wei-jun, XIONG Ying. Brown algae based new sorption material for fractional recovery of molybdenum and rhenium from wastewater [J]. Chemical Engineering Journal, 2015, 273: 231−239.
[30] BEUKENKAMP J, HERRINGTON K D. Ion-exchange investigation of the nature of titanium(IV) in sulfuric acid and perchloric acid [J]. Journal of the American Chemical Society, 1960, 82: 3025−3031.
[31] BAILLON F, PROVOST E, FURST W. Study of titanium(IV) speciation in sulphuric acid solutions by FT−Raman spectrometry [J]. Journal of Molecular Liquids, 2008, 143: 8−12.
[32] SHAN Wei-jun, FANG Da-wei, ZHAO Zhi-yi, YUE Shuang, LOU Zhen-ning, XING Zhi-qiang, XIONG Ying. Application of orange peel for adsorption separation of molybdenum(VI) from Re-containing industrial effluent [J]. Biomass Bioenergy, 2012, 37: 289−297.

浸渍二(2-乙基己基)磷酸的海藻酸钙微球去除和回收高硫铝土矿浸出液中的微量钛(IV)

娄振宁[1,2]，肖 欣[2]，熊 英[2]，翟玉春[1]

1. 东北大学 冶金学院，沈阳 110819；
2. 辽宁大学 化学院，沈阳 110036

摘 要：高硫铝土矿硫酸焙烧的浸出液中含有高浓度的铝，同时存在一定浓度的铁和钛。以生物质海藻为原料，用萃取剂二(2-乙基己基)磷酸(D2EHPA)经过简单浸渍，制备海藻酸钙微球吸附剂(CA-P204)用于去除高硫铝土矿浸出液中的钛。红外光谱和 X 射线光电子能谱表征证明，吸附机理为阳离子交换和螯合作用。柱实验结果表明：CA-P204 可从含有 Ti(IV)−Al(III)−Fe(III)的高硫铝土矿浸出液中去除钛，当 pH=1.0 时去除率可达 95%，对 Ti(IV) 的最大吸附量为 66.79 mg/g。3 次连续的吸附−脱附实验证明，吸附剂 CA-P204 具有较好的可再生性。该方法具有操作简单、价格低廉、没有其他废物排放等优点，同时 CA-P204 是一个可用于从高硫铝土矿的浸出液中除钛，具有良好应用前景、高效和经济性的吸附剂。

关键词：钛；D2EHPA；海藻酸钙微球；高硫铝土矿

(Edited by Xiang-qun LI)